SUPPLEMENTAL MATERIALS

TITLE: Pathogenic lymphangiogenesis promotes autoimmune valvular carditis

AUTHORS: Victoria Osinski, PhD[1]*, Amritha Yellamilli, MD, PhD[2,3]*, Maria M. Firulyova, MS[4,5], Jennifer L. Auger, BA[1], Lee A. Meier, PhD[1,3], Jessica L. Faragher, BS[1], Aubyn Marath, MBBS, MS[6], Rochus Voeller, MD[7], Konstantin Zaitsev, MS[5], Bryce A. Binstadt, MD, PhD[1]
*Authors contributed equally to this work

AUTHOR AFFILIATIONS*:*
1. Department of Pediatrics and Center for Immunology, University of Minnesota, Minneapolis, MN 55455
2. Department of Pediatrics, Stanford School of Medicine, Palo Alto, CA 94304
3. Medical Scientist Training Program, University of Minnesota Medical School, Minneapolis, MN 55455
4. Almazov National Medical Research Centre, Saint-Petersburg, Russia
5. Computer Technologies Laboratory, ITMO University, Saint Petersburg, Russia
6. CardioStart International, Tampa, FL 33619
7. Department of Surgery, University of Minnesota, Minneapolis, MN 55455

In this document:

SUPPLEMENTAL METHODS

Whole mount imaging of mitral valves

Hearts from C57Bl/6 and K/B.g7 were harvested and fixed in 4% paraformaldehyde for 2 hours at room temperature. Following PBS washes, the apex and ventral wall of each heart was removed to expose the mitral valves. Hearts were then permeabilized and blocked overnight at 4°C in PBS with 5% normal donkey serum (NDS) and 1% Tween-20. Following PBS washes, hearts were stained overnight at 4°C with primary antibodies in PBS with 5% NDS and 0.1% Tween-20. Hearts were then washed with PBS and stained with secondary antibodies for 4-6 hours at room temperature.

After thorough washing in PBS, the hearts were dehydrated by incubating tissue for 45 minutes each in 70%, 90%, 95%, 98%, and 2x 100% ethanol at room temperature. Tissues were then transferred into methyl salicylate and incubated at room temperature overnight (or longer) until tissues were cleared. Hearts were then mounted in methyl salicylate for imaging. Z stacked tile scans of mitral valves were acquired on the Leica Stellaris 8 using the 10x and 16x objectives. Images were acquired and stitched using the LasX (Leica) software. Image processing was conducted using Imaris software (Oxford Instruments).

Ki67 staining for flow cytometry

Mitral valves were harvested and digested as specified in the “scRNA sequencing: Tissue processing and sequencing” section of the Methods. Following ACK lysis and a final wash and spin, cells were stained with an antibody against CD16/32 (TONBO 70-0161) for 5 minutes on ice before adding antibodies specific for extracellular proteins for 30 minutes on ice. The antibodies used were CD11b-BV421 (Clone M1/70, BioLegend 101235), CD45.2-BV605 (Clone 104, BioLegend 612778), CD64-BV786 (Clone X54-5/7.1, BioLegend 741024), LYVE1-AF488 (Clone ALY7, ThermoFisher 53-0443), Feeder cells-PE (Clone mEF-SK4, Miltenyi Biotec 130-120-166), and CD31-PE-Cy7 (Clone 390, eBioscience 25-0311). Cells were then washed with PBS and stained with a fixable viability dye (Ghost Dye Red 780, TONBO 13-0865) for 20 minutes on ice. Following a wash with FACS buffer (2% BSA in PBS), the eBioscience Foxp3/Transcription Factor Buffer set (Invitrogen 00-5523-00) was used to stain for Ki67. Cells were fixed and permeabilized using the Fixation/Permeabilization buffer on ice for 30 minutes. Following washes with Permeabilization buffer, cells were incubated with a Ki67-AF647 antibody (Clone SolA15, eBioscience 51-5698) at room temperature for 1 hour. Cells were then washed with Permeabilization buffer and resuspended in FACS buffer for data acquisition. Cells were run on the CyTek Aurora and data analyzed using FlowJo (version 10, BD Biosciences).

Supplemental Tables

Table S1: Genotypes and sexes of lineage-traced mice used in this study.

	Number of males (M) and females (F)	
Age	**B.g7 *Cdh5*-creER^{T2} ROSA$^{mTmG/+}$**	**K/B.g7 *Cdh5*-creER^{T2} ROSA$^{mTmG/+}$**
4 weeks	3M, 2F	1M, 4F
8 weeks	2F	3M, 2F
12 weeks	3M, 4F	3M, 3F
20 weeks	3M, 2F	4M, 3F

Table S2: Antibodies used in this study. Table reports the antigen-specificity, host species, clone, company and dilution of each antibody used for histology in this study.

Antigen	Species	Catalog #	Company	Conjugation
Primary antibodies				
αSMA	Mouse	NBP2-33006AF594	Novus Biologicals	AF594
CCL21	Mouse	AF457-SP	R&D	None
CD31	Mouse	DIA-310	Dianova	None
CD45	Mouse	109814	Biolegend	APC
CD68	Mouse	137002	Biolegend	None
CD163	Human	MA5-11458	Invitrogen	None
LYVE1	Mouse	ab14917	Abcam	None
LYVE1	Human	AF2089	R&D	None
Periostin	Mouse	AF2955	R&D	None
Podoplanin	Human	916601	Biolegend	None
Prox1	Mouse/Human	ab199359	Abcam	None
VEGFR3	Mouse	AF743-SP	R&D	None
VEGFR3	Human	AF349	R&D	None
VWF	Mouse/Human	PA5-16634	Invitrogen	None
Secondary antibodies				
Mouse IgG	Donkey	715-585-150	Jackson ImmunoResearch	AF594
Rabbit IgG	Donkey	711-605-152	Jackson ImmunoResearch	AF647
Rat IgG	Donkey	712-605-153	Jackson ImmunoResearch	AF647
Mouse IgG	Donkey	715-605-151	Jackson ImmunoResearch	AF647
Rabbit IgG	Donkey	711-545-152	Jackson ImmunoResearch	AF488
Mouse IgG	Donkey	715-165-150	Jackson ImmunoResearch	Cy3
Goat IgG	Donkey	705-165-003	Jackson ImmunoResearch	Cy3
Goat IgG	Donkey	705-585-003	Jackson ImmunoResearch	AF594
Goat IgG	Donkey	705-605-147	Jackson ImmunoResearch	AF647
Rabbit IgG	Donkey	711-585-152	Jackson ImmunoResearch	AF594
Rat IgG	Goat	405410	Biolegend	Dylight 594

Table S3: Gene profiles of each cell cluster in murine mitral valves. Mitral valve cells were clustered into 14 clusters numbered 0-13. Samples from 3-, 8-, and 25-week-old BxN and K/BxN mitral valves were pooled for this analysis. The “Key” tab labels each cluster for reference. Differentially expressed genes with an adjusted *p*-value

of less than 0.05 for each cluster were identified using limma. Each cluster was compared to all other clusters pooled together and the differentially expressed genes for that cluster are separated into individual tabs in the table.

See separate file: Supp Table 3.xlsx

Table S4: Gene profiles of each VEC cluster. VECs were clustered into 7 unique endothelial clusters. The "Key" tab provides labels for each cluster for reference. Differentially expressed genes with an adjusted *p*-value of less than 0.05 for each cluster were identified using limma. Each cluster was compared to all other clusters pooled together and the differentially expressed genes for that cluster are separated into individual tabs in the table. The genes enriched in VECs, Lymph-VECs, and Coapt-VECs from Hulin *et al* and used in Figure S3H are included in this table in a separate table labeled "Hulin et al Gene lists".

See separate file: Supp Table 4.xlsx

Table S5: Gene profiles and enriched pathways of each Lymph-VEC cluster. Lymph-VEC Clusters 1 and 5 were compared to one another using limma to identify genes significantly upregulated in each cluster (*p*-value < 0.01). Differentially expressed genes (DEGs) are listed in the "DEGs" tab. GO Biological Processes pathways enriched in each cluster were determined using Enrichr and all DEGs reported. The pathways enriched in Clusters 1 and 5 are reported on tabs "cl1-enriched-pathways" and "cl5-enriched-pathways", respectively.

See separate file: Supp Table 5.xlsx

Table S6: Genes differentially expressed along the K/BxN Lymph-VEC trajectory. Lymph-VEC Clusters 1 and 5 were subjected to trajectory analysis using slingshot (Figure 3C) and tradeseq was used to identify genes differentially expressed at the start and end of the trajectory by applying the start-vs-end test. Differentially expressed genes with an adjusted *p*-value of less than 0.05 are presented and a positive log-fold-change (logFClineage) indicates greater expression of that gene at the end of the trajectory. Up- and down-regulated genes were each used to identify enriched GO Biological Processes along the trajectory using Enrichr and are reported in two additional tabs in this table. The top 10 pathways from each tab are reported in Figure 3E.

See separate file: Supp Table 6.xlsx

Table S7: Human mitral valve sample patient information. The age, sex, and diagnosis of the individuals from which each mitral valve sample was isolated is listed. Controls required mitral valve replacements or repairs due to non-rheumatic disease.

Sample	Diagnosis	Age	Sex	Source
Control #1	Alcoholic Pulmonary Hypertension	60	F	CardioStart Study
Control #2	Fibrosis with focal myxoid change and calcification	84	M	UMN CTSI Biorepository
Control #3	Nonrheumatic mitral valve regurgitation, Chronic diastolic heart failure	48	F	UMN CTSI Biorepository
Case #1	Severe mitral valve stenosis and regurgitation, moderate tricuspid valve regurgitation	27	F	CardioStart Study
Case #2	Severe mitral valve stenosis, moderate mitral valve and aortic valve regurgitation, severe pulmonary hypertension	31	M	CardioStart Study
Case #3	Rheumatic valve disease - Mitral valve stenosis	53	M	CardioStart
Case #4	Rheumatic heart affected valve	37	F	CardioStart
Case #5	Rheumatic heart affected valve	24	M	CardioStart
Case #6	Mitral valve regurgitation	58	M	CardioStart
Case #7	Mitral valve regurgitation, rheumatic heart disease, shortness of breath	17	M	CardioStart
Case #8	Severe Mitral Regurgitation	48	F	CardioStart Study
Case #9	Severe Mitral Regurgitation	45	F	CardioStart Study

Supplemental Figure Legends

Figure S1. Lineage-tracing and development of autoantibodies, arthritis and valvular carditis in K/B.g7 Cdh5-CreER^{T2} ROSA$^{mTmG/+}$ mice. A. Bar graph of anti-GPI IgG levels in K/B.g7 Cdh5-CreER^{T2} ROSA$^{mTmG/+}$ mice at 4-, 8-, 12-, and 20-weeks of age. Levels were normalized to an 8-week-old K/B.g7 control sample. **B.** Weekly arthritis scores and hind ankle width measurements of K/B.g7 Cdh5-CreER^{T2} ROSA$^{mTmG/+}$ mice analyzed at time points 8-, 12-, and 20-weeks. Arthritis scores report the sum of arthritis severity scores per paw. Ankle thickness measurements are the sum of both hind ankles minus the initial ankle thickness measurements made at 3 weeks of age. The mean scores and widths for mice per age group are displayed with error bars reporting standard deviation. **C.** Bar graph reporting the mitral valve thickness of each B.g7- or K/B.g7 Cdh5-CreER^{T2} ROSA$^{mTmG/+}$ mouse per age group. MV thickness reports the average of maximum thickness measured in 5 images of the valves per mouse. Statistics calculated using Mann Whitney U tests. **D.** Scatter plot of the number of mGFP+ interstitial vessels and valve thickness per Cdh5-CreER^{T2} ROSA$^{mTmG/+}$ mouse. The x-axis is reported on a log scale to better resolve individual data points. *P*- and r^2 values were calculated using a simple linear regression. **E.** Representative images of mGFP, mTom, and DAPI staining for each age and genotype used for lineage-tracing experiments. Lowercase letters in lower magnification images indicate the corresponding higher magnification image of each image. Scale bars are 100 µm.

Figure S2. Vehicle-treated Cdh5-creER^{T2} ROSA$^{mTmG/+}$ mitral valves remain unlabeled with mGFP. A. To address the potential for mGFP-labeling of cells in the absence of tamoxifen, a K/B.g7 Cdh5-creER^{T2} ROSA$^{mTmG/+}$ mouse was treated with corn oil (vehicle) for three consecutive days at 3 weeks of age. The heart was then harvested at 12 weeks of age to assess mGFP signal by microscopy. **B.** Sections from a tamoxifen-treated B.g7 Cdh5-creER^{T2} ROSA$^{mTmG/+}$ mouse (treated and harvested on the same timeline as A) was used as a positive control. **C.** Microscopy of the vehicle-treated heart reveals no mGFP labeling in the mitral valve. The bottom row of images is a higher magnification of the image found in the white box in the center row of images. Settings for acquiring and processing images in B and C were identical to appropriately compare mGFP signal. Scale bars are 50 µm.

Figure S3. Single cell sequencing analysis approach and selected cluster merging. A. Experimental schematic outlining the steps taken to process and analyze single cell sequencing data of BxN and K/BxN valves. **B.** Original and manually merged UMAP plots of all the MV clusters from pooled BxN and K/BxN samples. **C.** Original and manually merged VEC UMAPs overlaid with cluster labels.

Figure S4. Whole mount imaging of mitral valves reveals LYVE1+ lymphatic vessels in inflamed mitral valves. A-B. Hearts from 13-week old K/B.g7 (**A**) and Bl/6 (**B**) mice were harvested and stained for CD31 and LYVE1 for deep tissue imaging. Lower magnification single channel and merged images of the valves are found in the top 3 rows of images. There, dotted lines outline the mitral valve, A indicates atrium, and V indicates ventricle. Scale bars are 200 µm. In the lower panels, higher magnification of the images located within the white boxes are shown. The dotted lines in the K/B.g7 valve outline LYVE1+ vessels, while the arrows in the Bl/6 valve indicate LYVE1+ cells that are likely macrophages.

Figure S5. Proliferating Lymph-VECs increase to a greater extent in K/B.g7 valves compared to uninflamed controls. A. Gating strategy for identifying CD45-CD31+ VECs and CD45-CD31+LYVE1+ Lymph-VECs and the Ki67+ subset of each. **B.** The proportion of Ki67+ VECs (% Ki67+ VECs), total number of VECs per valve (# VECs), and number of Ki67+ VECs per valve (# Ki67+ VECs) were quantified in 5- and 12-week old uninflamed Bl/6 and inflamed K/B.g7 mice. **C.** The proportion of Ki67+ Lymph-VECs (% Ki67+ Lymph-VECs), total number of Lymph-VECs per valve (# Lymph-VECs), and number of Ki67+ Lymph-VECs per valve (# Ki67+ Lymph-VECs) were quantified in 5- and 12-week old uninflamed Bl/6 and inflamed K/B.g7 mice. **D.** The proportional increase in number of VECs or Lymph-VECs from 5- to 12-week old valves in uninflamed (Bl/6) and inflamed (K/B.g7) mice was determined. Statistics were calculated using Mann-Whitney U tests (**B,C**) and 2-way ANOVA (**D**).

Figures S6. αSMA expression is not detected in the mitral valve. **A-D.** Immunostaining of αSMA in the heart of a 12-week-old K/B.g7 Cdh5-CreER^{T2} ROSA$^{mTmG/+}$ mouse. Positive staining was not detected in the mitral valve (**A**), but was in the aorta (**B**) and arteries of the left ventricle (**C**) and right ventricle (**D**). Scale bars are 100 µm on main, merged panels, and 50 µm on inset panels. LA, left atrium; LV, left ventricle; Ao, aorta; Art, artery.

Figure S7. mGFP+ cells do not express CD68 in the mitral valve. A-C. Immunostaining of CD68 and LYVE1 in the hearts of an 8-week-old B.g7 Cdh5-CreER^{T2} ROSA$^{mTmG/+}$ (**A**), and 8- and 12-week-old K/B.g7 Cdh5-CreER^{T2} ROSA$^{mTmG/+}$ mice (**B,C**) reveals the existence of mGFP+LYVE1+ lymphatics (arrows) and LYVE1+CD68+ macrophages (arrow heads) in the mitral valve that are mGFP^{neg}. Scale bars are 50 μm in upper left panels and 25 μm in lower right panels per mouse. LA, left atrium; LV, left ventricle.

Figure S8. Typical marker transcripts for endothelial cell and macrophage markers are isolated to their respective cell populations by scRNA seq. Endothelial (original Clusters 3, 7, and 11, Figure 2A) and myeloid cells (original cluster 4, Figure 2A) were isolated from total sequenced mitral valve cells and re-clustered as individual cell populations. Transcripts upregulated in either macrophages (*Ptprc*, *Itgam*, *Fcgr1*, *Cd68*, *Adgre1*) or endothelial cells (*Pecam1*, *Cdh5, Erg*) were overlaid on both the myeloid and endothelial UMAP plots. *Lyve1*, which is found in both populations, was included as well. All UMAP plots show UMAP_2 on the Y axis, and UMAP_1 on the X axis, and relative gene expression levels scales.

Figure S9. Individual LYVE1+mGFP+ cells and vessels reside along the atrial side of the mitral valves. A. Paired bar graphs of the distance of interstitial LYVE1+mGFP+ vessels from the atrial surface and total valve thickness at the location of each vessel for 12- and 20-week old B.g7 and K/B.g7 lineage-traced mice. Each data point represents a different mouse and lines connect paired metrics per mouse. **B.** Bar graph of the number of LYVE1+mGFP+ cells located on the atrial surface of the MV of 4- and 8-week old B.g7 and K/B.g7 lineage-traced mice. No LYVE1+mGFP+ cells were identified on the ventricular surface of the MV. **C.** Example image of a 4-week-old K/B.g7 lineage-traced mitral valve with surface LYVE1+mGFP+ cell and emergent LYVE1+mGFP+ vessel. Inset image #1 shows a surface LYVE1+mGFP+ cell on the atrial surface with an arrow delineating the cell. Inset image #2 shows an emergent LYVE1+mGFP+ vessel with an arrow delineating the vessel. **D.** Example image of an 8-week-old K/B.g7 lineage-traced mitral valve with emergent LYVE1+mGFP+ vessels, which are enlarged in image insets #1 and #2. **C,D.** A: atrium, V: ventricle. Scale bars are 50 μm.

Figure S10. LYVE1 staining and mGFP labeling of cells and vessels in healthy and inflamed valves. A. Example image of a B.g7 lineage-traced valve with an interstitial LYVE1+mGFP+ vessel located near the atrial side. Scale bar is 50 μm. White box delineates location of magnified images in lower panel, which highlight mGFP (green), LYVE1 (white), and merged staining left to right. **B.** Example images of a B.g7 lineage-traced (left) and K/B.g7 lineage-traced (right) valve with LYVE1^{neg}mGFP+ interstitial vessels. White boxes in each upper panel delineate the location of magnified images in the lower panels, which highlight mGFP (green), LYVE1 (white), and merged staining left to right. **C.** Scatter plots of the number of LYVE1+mGFP+ (top) or LYVE1^{neg}mGFP+ (bottom) vessels plotted against the valve thickness for the corresponding sample in 4-, 8-, 12-, and 20-week old B.g7 and K/B.g7 lineage-traced valves. The valve thickness axis is plotted on a log2 scale to better resolve individual data points. *P*- and r^2 values were calculated using a simple linear regression. **D.** Example image of a LYVE1^{neg}mGFP+ individual cell located in the interstitium of a K/B.g7 lineage-traced valve. The left panel shows the merged image with LYVE1 (white), mGFP (green), mTom (red), and DAPI (blue) staining, while the right panel shows LYVE1 staining alone. The inset panels in the upper right-hand corner show a higher magnification of the mGFP+ cell. **E.** A bar graph reporting the number of LYVE1^{neg}mGFP+ cells located in the interstitium of 4-, 8-, 12-, and 20-week old B.g7 and K/B.g7 lineage-traced valves. **A,B,D.** A: atrium, V: ventricle. Scale bars are 50 μm.

Figure S11: Trajectory analysis of total VECs. A. Example image of a mGFP+LYVE1+ vessels localized to the atrial side of an inflamed valve in a 12-week old K/B.g7 *Cdh5*-lineage-traced mouse. Scale bar is 50 μm. **B.** Trajectory plot of all VECs from BxN and K/BxN samples pooled together and overlaid with cell clusters from endothelial-specific clustering. **C.** Genes specific for Lymph-VECs (*Flt4*), endocardial VECs (*Npr3*), coaptation VECs (*Hapln1*), PROX1+LYVE1^{neg} VECs (*Lsamp*), arterial VECs (*Sox17*), and proliferating VECs (*Mki67*) overlaid on the trajectory plot.

Figure S12. Blockade of VEGFR3 does not alter development of autoantibody generation or arthritis development. A. Expression of Flt4 in total MV cells overlaid on UMAP plots from scRNA seq data. **B.** Plotted average weekly change in ankle width measurements (left) and arthritis scores (right) of control (n = 10) or MAZ51-treated (n = 9) mice before and during treatment. Scoring is performed on a scale of 0 to 3 per limb with 0 indicating no arthritis and 3 indicating severe arthritis. **C.** The anti-GPI IgG titers of control (n = 10) or MAZ51-treated (n = 9) mice at the end of treatment. IgG levels were normalized to an 8-week-old K/B.g7 control sample. **D-E.** Circulating levels of IL-6 (**D**) and TNF (**E**) were measured in the plasma of treated mice using ELISA. **F.** Hearts from MAZ51- and control-treated hearts were stained with antibodies specific for CD31 and VEGFR3 to quantify lymphatic vessels. **G-H.** The number of VEGFR3+ vessels in the left atrium (LA, **G**), left ventricle (LV, **H**), and right ventricle (RV, **H**) were quantified and normalized to the area of tissue imaged. For the ventricles, the

number of lymphatics along the outer edge of the heart were normalized to the length of ventricle imaged (**H**, upper graph) and the total lymphatics were normalized to the area of tissue imaged (**H**, lower graph). Scale bars in **F** is 500 μm and in **G-H** are 50 μm. Statistics were calculated using Mann-Whitney U tests.

Figure S13. Lymphatic and macrophage markers in human mitral valve tissue. A. Examples of LYVE1+, VEGFR3+, and Podoplanin+ vessels in rheumatic (Case) valves. Arrows indicate lymphatic vessels in Case #2. Scale bars are 100 μm. **B.** VEGFR3, Podoplanin, and VWF staining in non-rheumatic (Control) valves. VWF+ blood vessels were identified in Control #1 and VEGFR3+ staining lacking vessel morphology was identified in Control #3. Scale bars are 100 μm. **C.** Immunostaining of LYVE1, macrophage marker CD163, and VWF in a non-rheumatic valve reveals LYVE1+CD163+ macrophages. A higher magnification of some of these LYVE1+ CD163+ macrophages is highlighted in the white, inset box of the merged image. Scale bar is 50 μm.

Figure S1

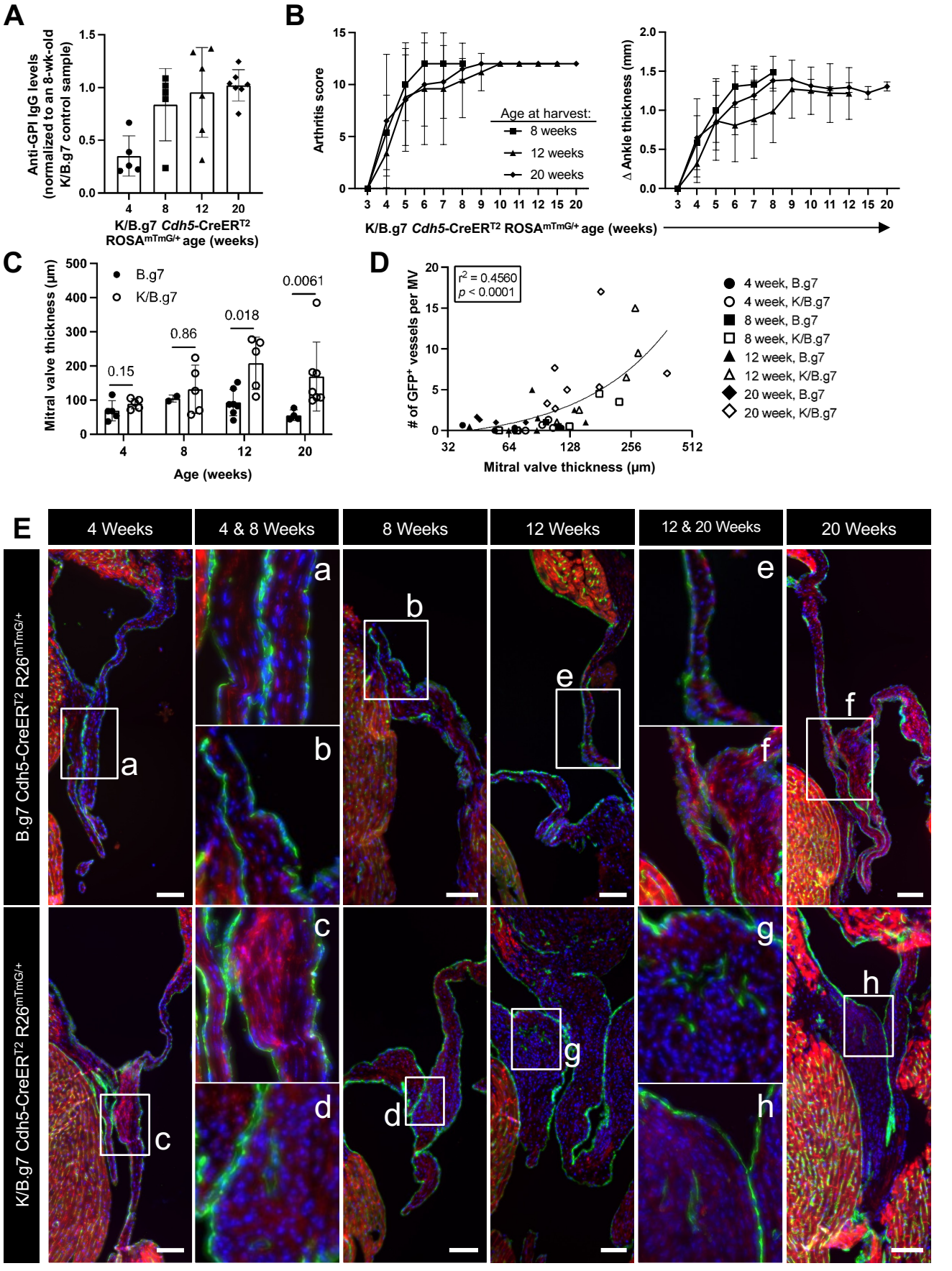
A
Anti-GPI IgG levels (normalized to an 8-wk-old K/B.g7 control sample)
K/B.g7 Cdh5-CreER^T2 ROSA^mTmG/+ age (weeks)
B
Arthritis score
Age at harvest:
8 weeks
12 weeks
20 weeks
Δ Ankle thickness (mm)
K/B.g7 Cdh5-CreER^T2 ROSA^mTmG/+ age (weeks)
C
Mitral valve thickness (μm)
B.g7
K/B.g7
0.15
0.86
0.018
0.0061
Age (weeks)
D
r^2 = 0.4560
p < 0.0001
# of GFP+ vessels per MV
Mitral valve thickness (μm)
4 week, B.g7
4 week, K/B.g7
8 week, B.g7
8 week, K/B.g7
12 week, B.g7
12 week, K/B.g7
20 week, B.g7
20 week, K/B.g7
E
4 Weeks
4 & 8 Weeks
8 Weeks
12 Weeks
12 & 20 Weeks
20 Weeks
B.g7 Cdh5-CreER^T2 R26^mTmG/+
K/B.g7 Cdh5-CreER^T2 R26^mTmG/+

Figure S2

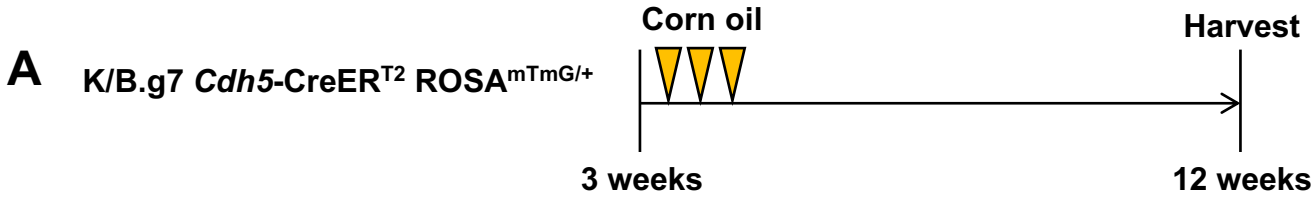
A
K/B.g7 Cdh5-CreER^T2 ROSA^mTmG/+
Corn oil
Harvest
3 weeks
12 weeks

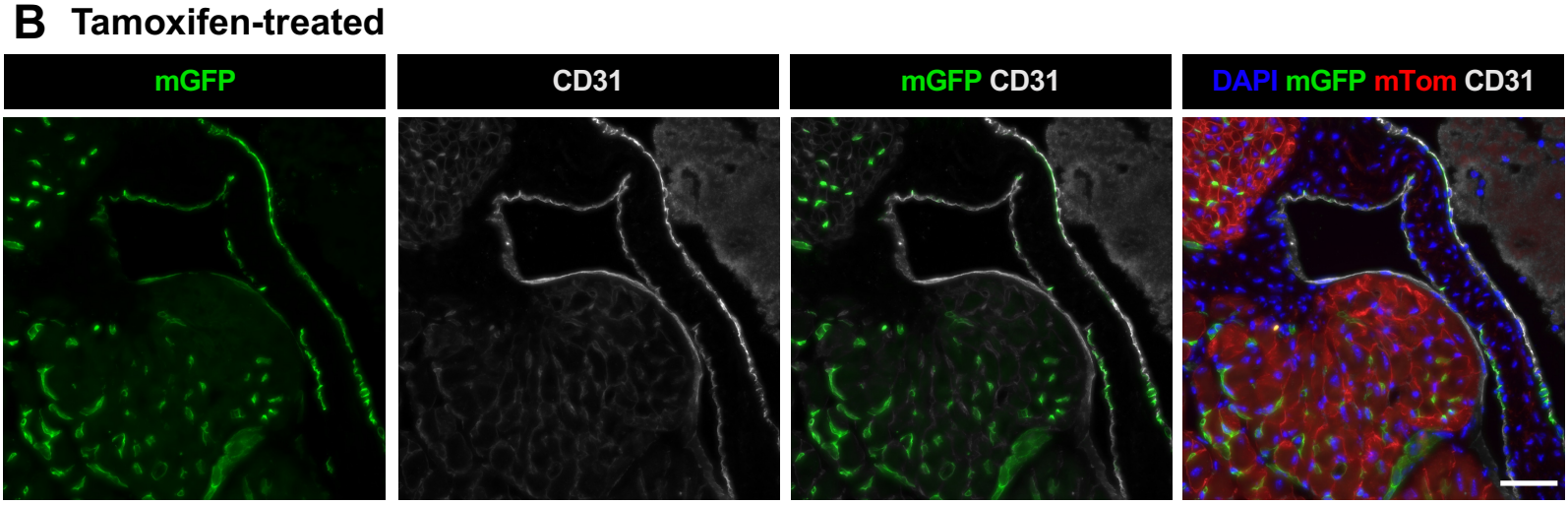
B Tamoxifen-treated
mGFP
CD31
mGFP CD31
DAPI mGFP mTom CD31

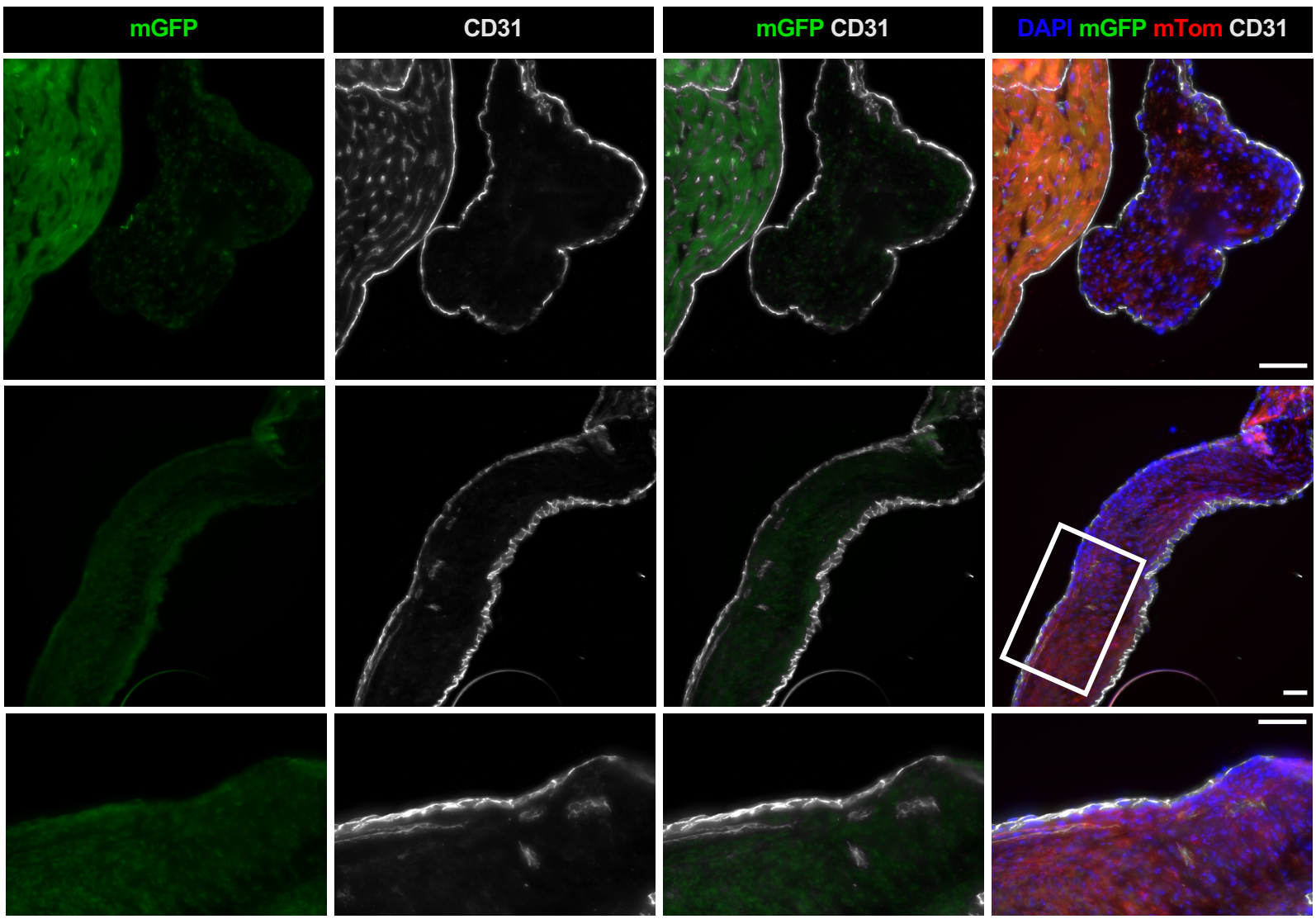
C Corn oil-treated
mGFP
CD31
mGFP CD31
DAPI mGFP mTom CD31

Figure S3

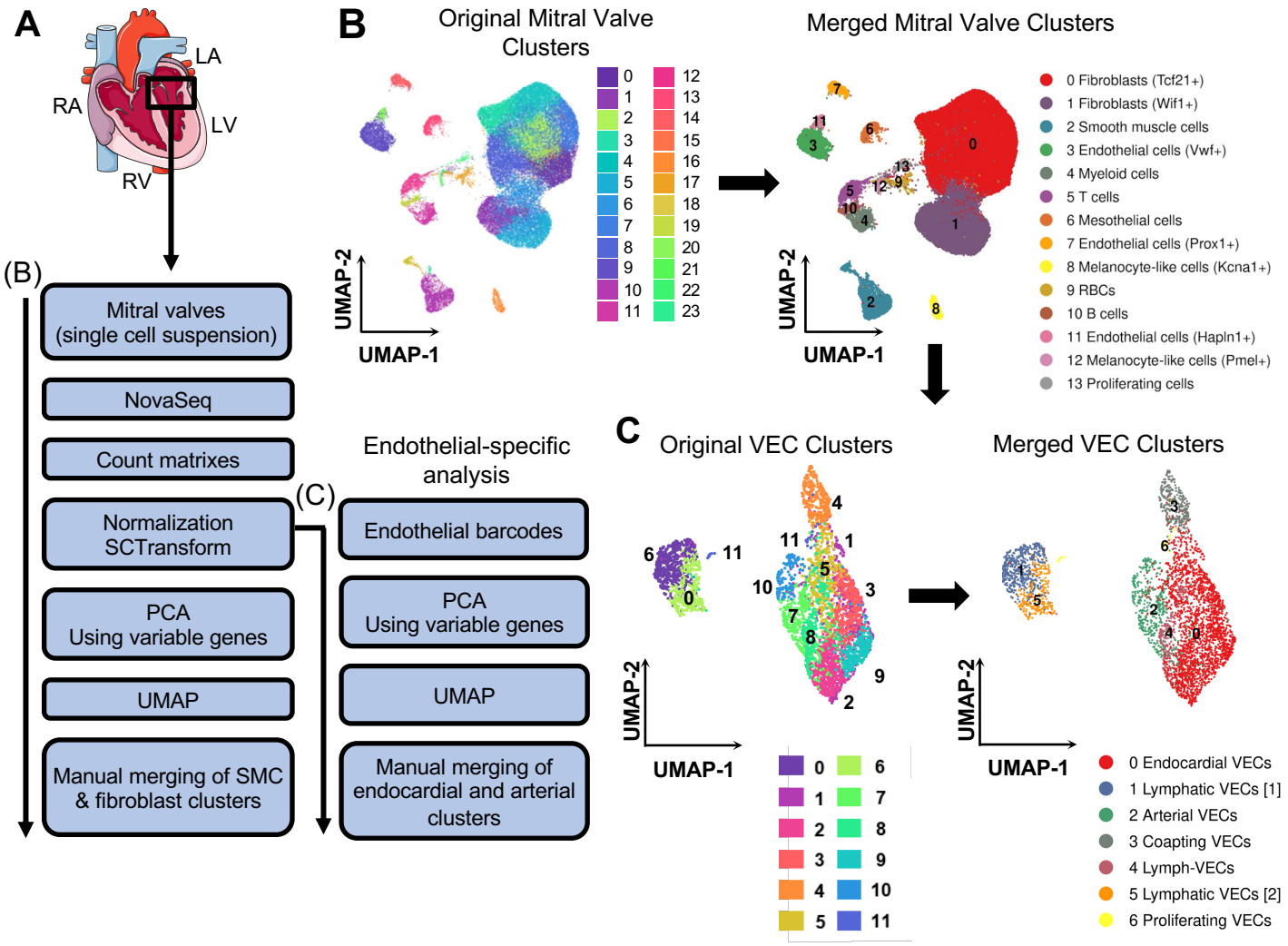
A
LA
RA
LV
RV
(B)
Mitral valves (single cell suspension)
NovaSeq
Count matrixes
Normalization SCTransform
PCA Using variable genes
UMAP
Manual merging of SMC & fibroblast clusters
(C)
Endothelial-specific analysis
Endothelial barcodes
PCA Using variable genes
UMAP
Manual merging of endocardial and arterial clusters
B
Original Mitral Valve Clusters
Merged Mitral Valve Clusters
UMAP-1
UMAP-2
0 Fibroblasts (Tcf21+)
1 Fibroblasts (Wif1+)
2 Smooth muscle cells
3 Endothelial cells (Vwf+)
4 Myeloid cells
5 T cells
6 Mesothelial cells
7 Endothelial cells (Prox1+)
8 Melanocyte-like cells (Kcna1+)
9 RBCs
10 B cells
11 Endothelial cells (Hapln1+)
12 Melanocyte-like cells (Pmel+)
13 Proliferating cells
C
Original VEC Clusters
Merged VEC Clusters
0 Endocardial VECs
1 Lymphatic VECs [1]
2 Arterial VECs
3 Coapting VECs
4 Lymph-VECs
5 Lymphatic VECs [2]
6 Proliferating VECs

Figure S4

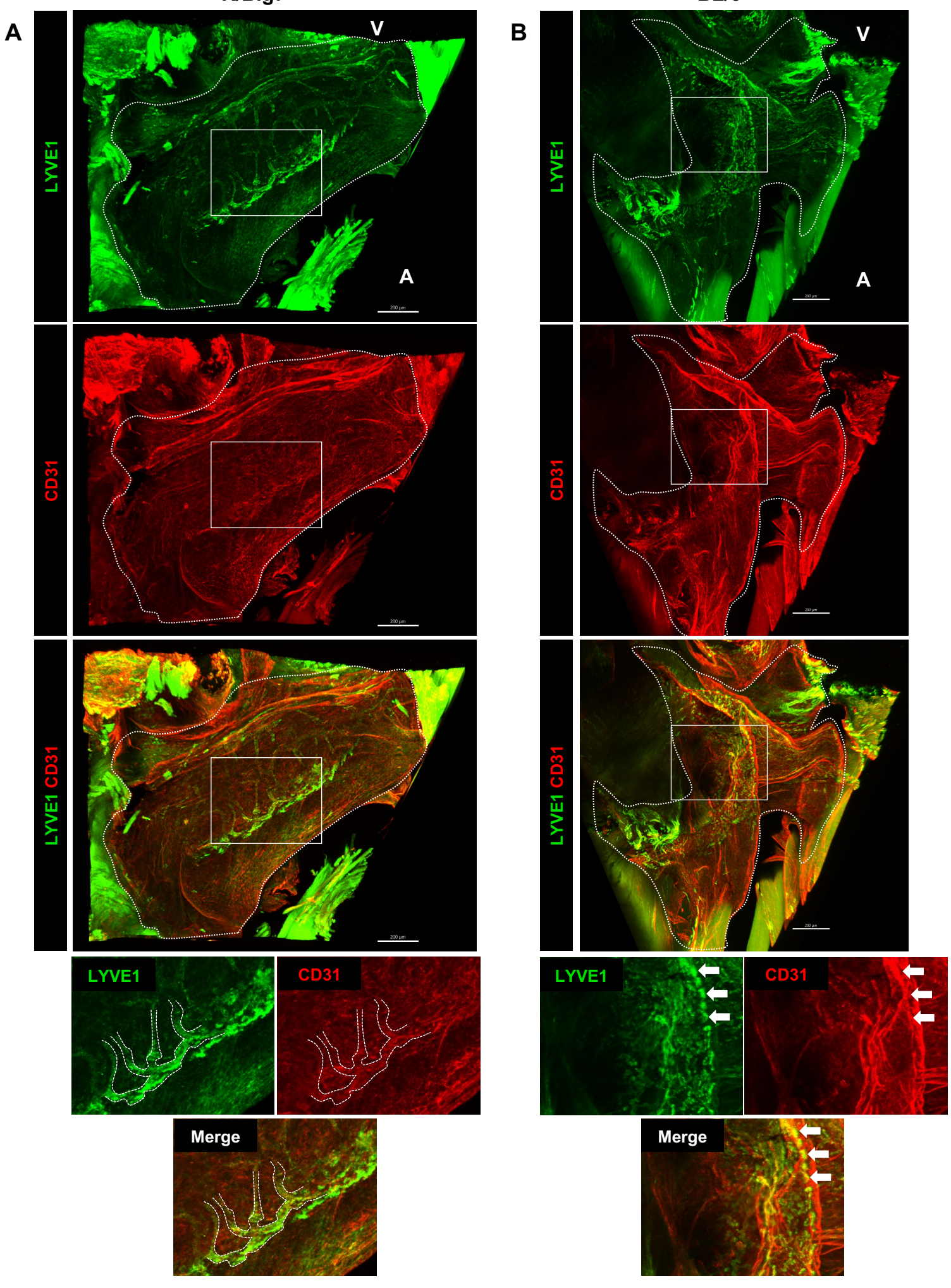

Figure S5

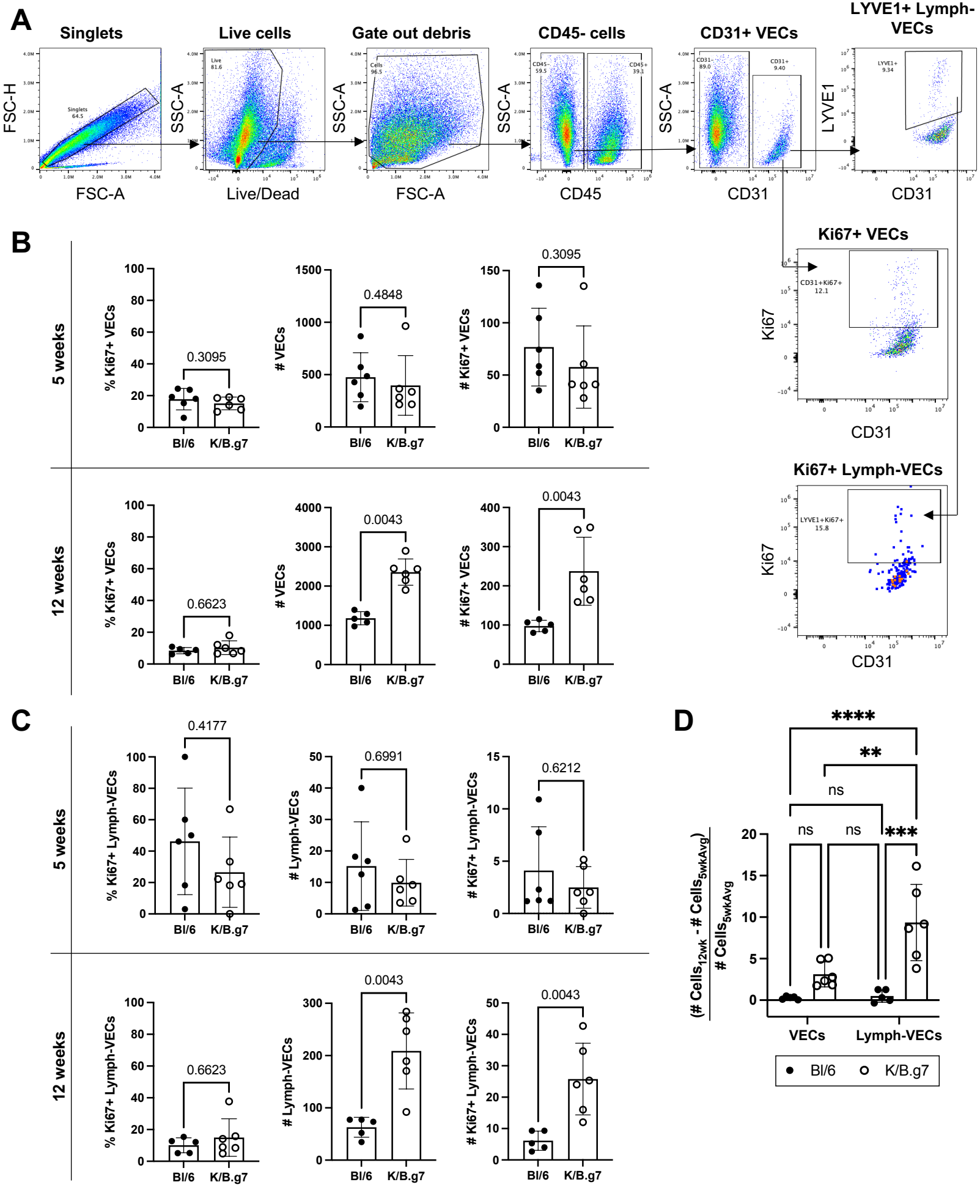
A
Singlets
Live cells
Gate out debris
CD45- cells
CD31+ VECs
LYVE1+ Lymph-VECs
FSC-H
FSC-A
SSC-A
Live/Dead
CD45
CD31
LYVE1
Singlets 64.5
Live 81.6
Cells 96.5
CD45- 59.5
CD45+ 39.1
CD31- 89.0
CD31+ 9.40
LYVE1+ 9.34
B
5 weeks
12 weeks
% Ki67+ VECs
# VECs
# Ki67+ VECs
Bl/6
K/B.g7
0.3095
0.4848
0.3095
0.6623
0.0043
0.0043
Ki67+ VECs
CD31+Ki67+ 12.1
Ki67
CD31
Ki67+ Lymph-VECs
LYVE1+Ki67+ 15.8
C
% Ki67+ Lymph-VECs
# Lymph-VECs
# Ki67+ Lymph-VECs
0.4177
0.6991
0.6212
0.6623
0.0043
0.0043
D
(# Cells12wk - # Cells5wkAvg) / # Cells5wkAvg
****
**
ns
ns
ns
***
VECs
Lymph-VECs
Bl/6
K/B.g7

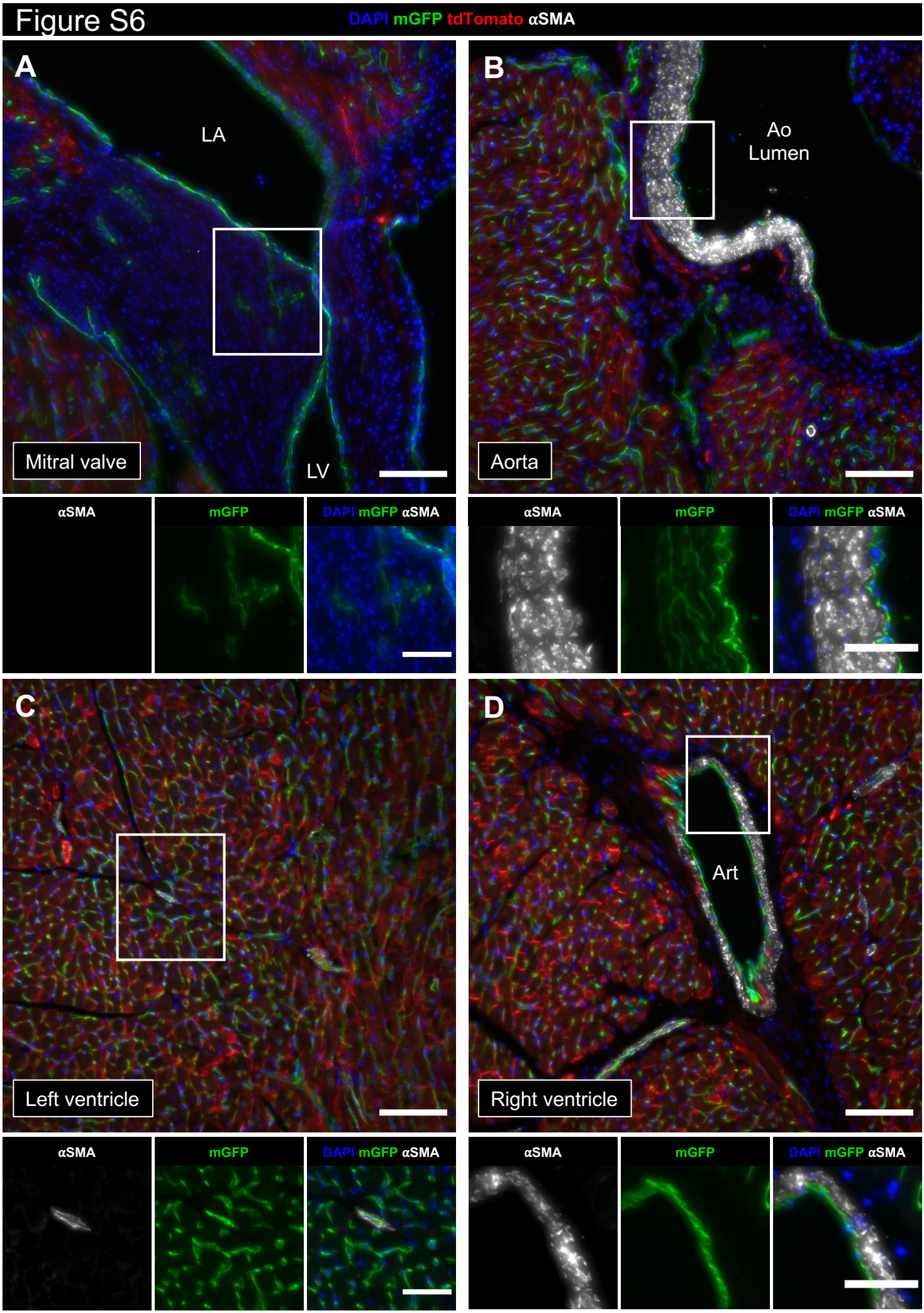
Figure S6
DAPI mGFP tdTomato αSMA
A
LA
Mitral valve
LV
B
Ao
Lumen
Aorta
αSMA
mGFP
DAPI mGFP αSMA
αSMA
mGFP
DAPI mGFP αSMA
C
Left ventricle
D
Art
Right ventricle
αSMA
mGFP
DAPI mGFP αSMA
αSMA
mGFP
DAPI mGFP αSMA

Figure S7

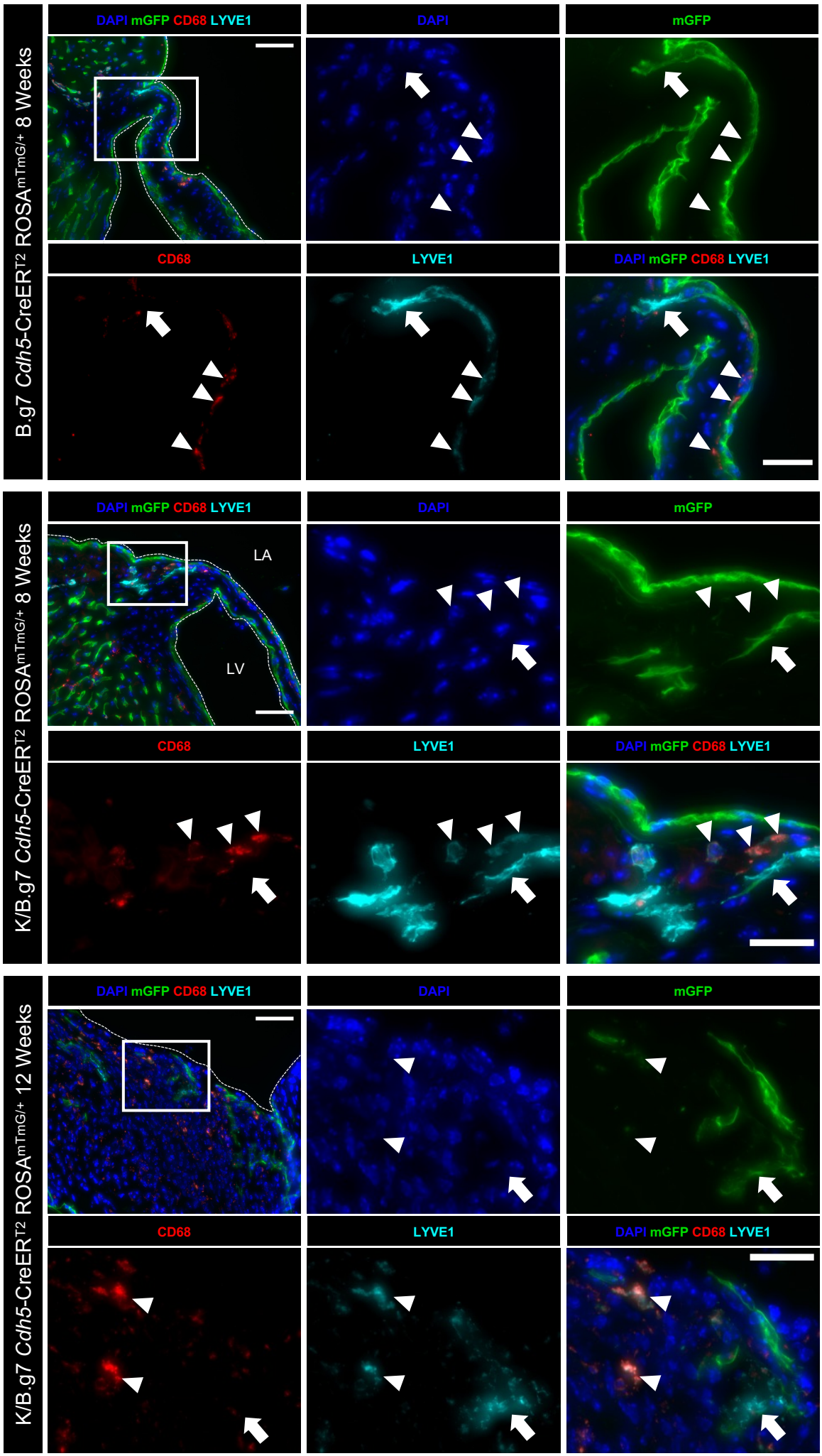
B.g7 Cdh5-CreER^{T2} ROSA$^{mTmG/+}$ 8 Weeks
K/B.g7 Cdh5-CreER^{T2} ROSA$^{mTmG/+}$ 8 Weeks
K/B.g7 Cdh5-CreER^{T2} ROSA$^{mTmG/+}$ 12 Weeks
DAPI mGFP CD68 LYVE1
DAPI
mGFP
CD68
LYVE1
DAPI mGFP CD68 LYVE1
LA
LV

Figure S8

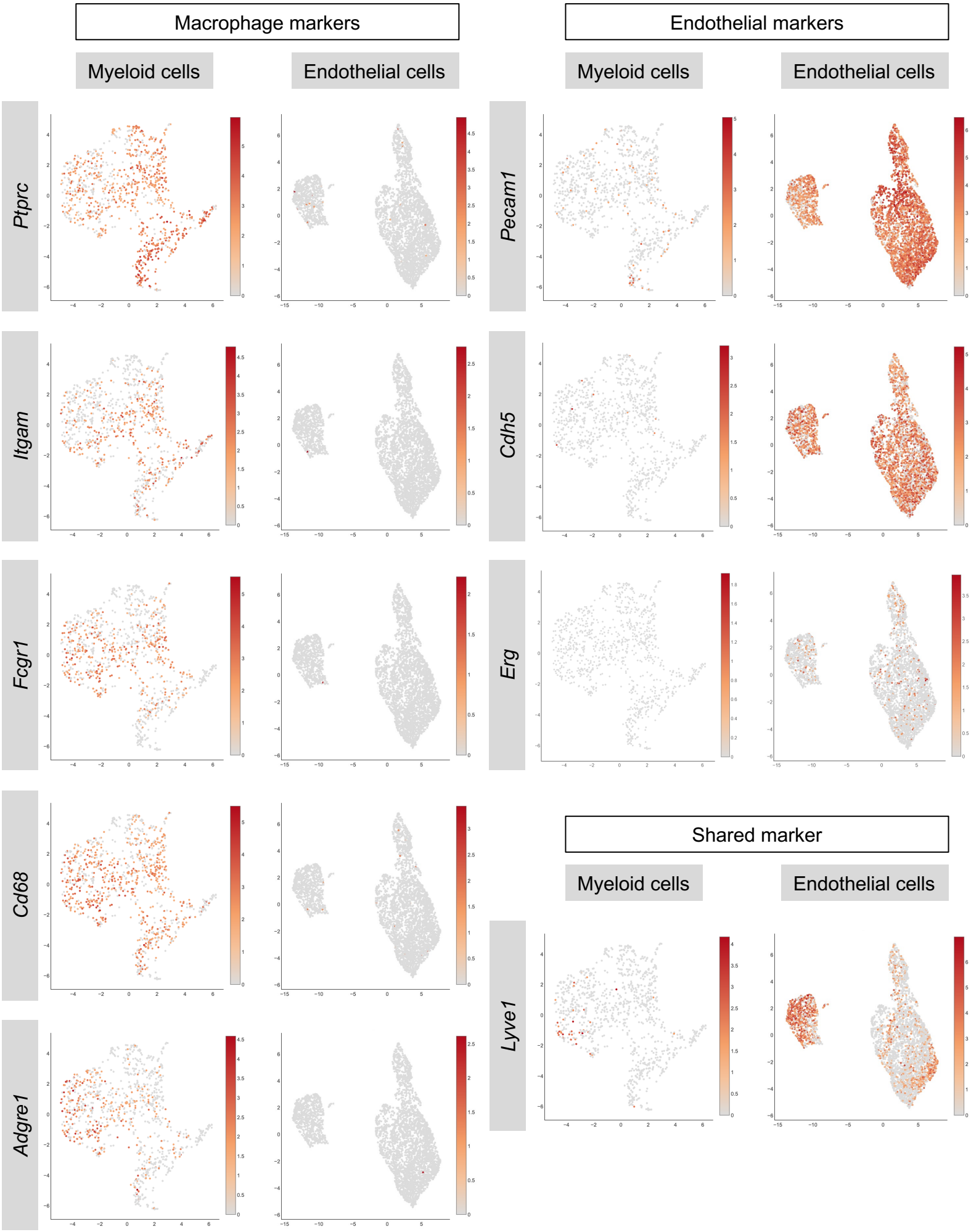
Macrophage markers
Endothelial markers
Myeloid cells
Endothelial cells
Myeloid cells
Endothelial cells
Ptprc
Pecam1
Itgam
Cdh5
Fcgr1
Erg
Cd68
Shared marker
Myeloid cells
Endothelial cells
Lyve1
Adgre1

Figure S9

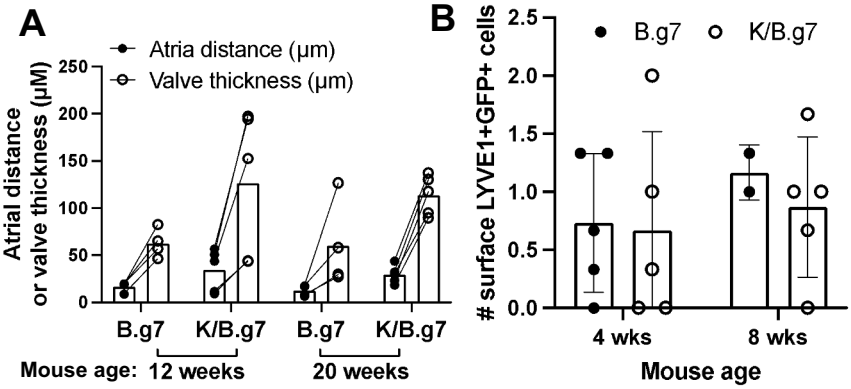
A
Atria distance (μm)
Valve thickness (μm)
Atrial distance or valve thickness (μM)
250
200
150
100
50
0
B.g7
K/B.g7
B.g7
K/B.g7
Mouse age:
12 weeks
20 weeks
B
B.g7
K/B.g7
surface LYVE1+GFP+ cells
2.5
2.0
1.5
1.0
0.5
0.0
4 wks
8 wks
Mouse age

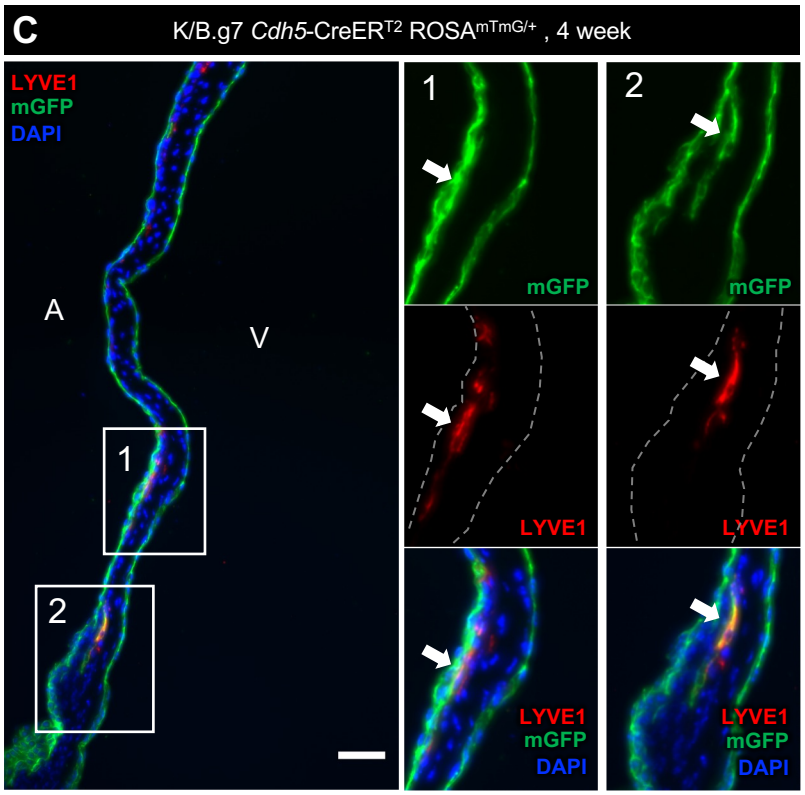
C
K/B.g7 Cdh5-CreERT2 ROSAmTmG/+ , 4 week
LYVE1
mGFP
DAPI
A
V
1
2
mGFP
LYVE1
LYVE1
mGFP
DAPI

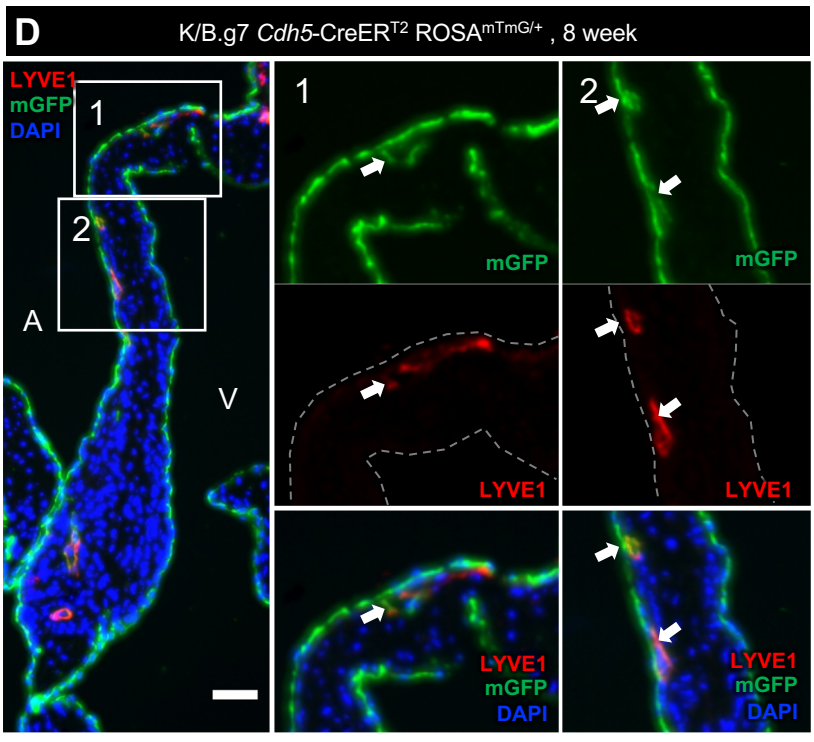
D
K/B.g7 Cdh5-CreERT2 ROSAmTmG/+ , 8 week
LYVE1
mGFP
DAPI
1
2
A
V
mGFP
LYVE1
LYVE1
mGFP
DAPI

Figure S10

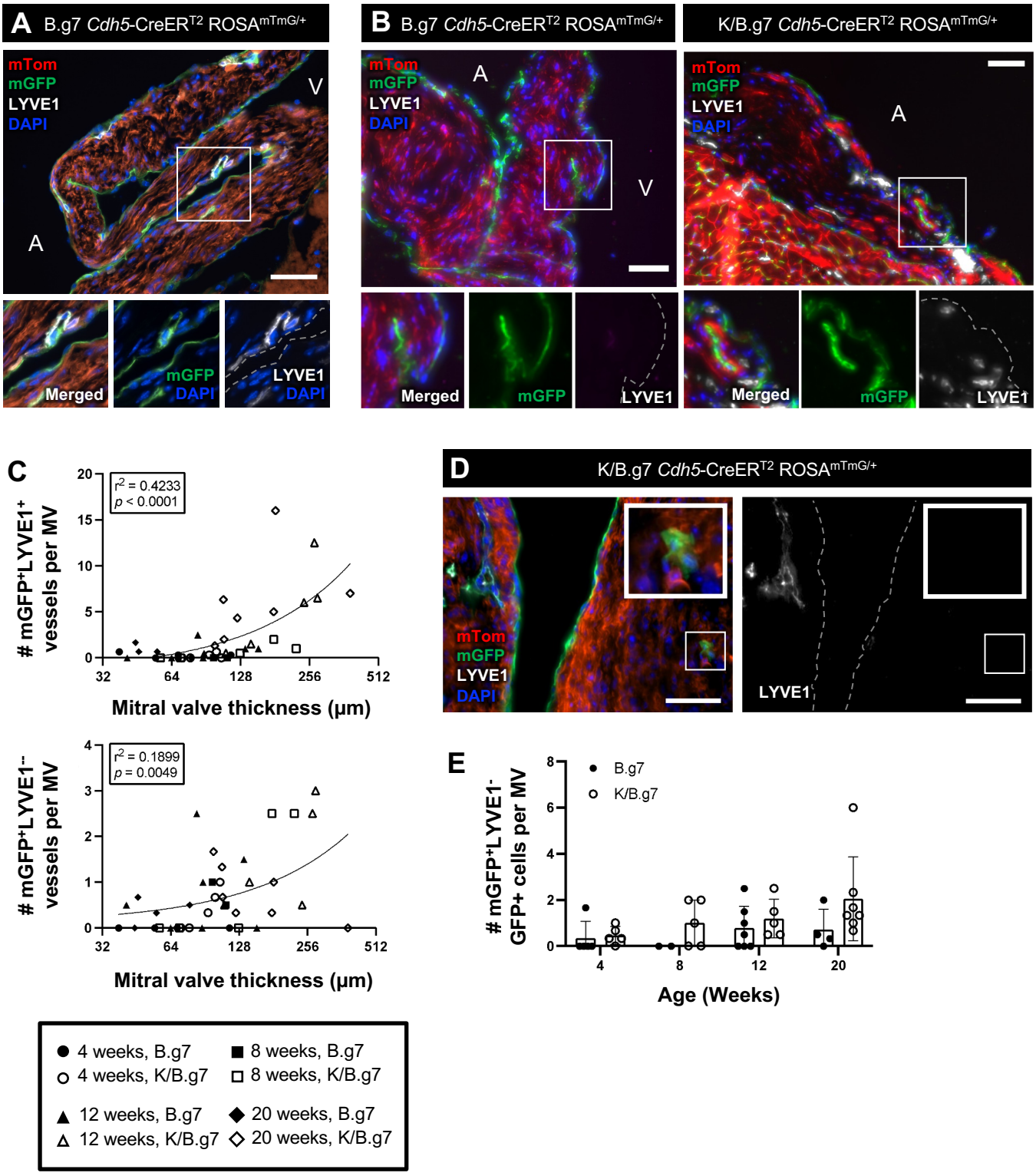
A B.g7 Cdh5-CreERT2 ROSAmTmG/+
mTom
mGFP
LYVE1
DAPI
V
A
Merged
mGFP
DAPI
LYVE1
B B.g7 Cdh5-CreERT2 ROSAmTmG/+
K/B.g7 Cdh5-CreERT2 ROSAmTmG/+
C
# mGFP+LYVE1+ vessels per MV
r2 = 0.4233
p < 0.0001
Mitral valve thickness (μm)
# mGFP+LYVE1- vessels per MV
r2 = 0.1899
p = 0.0049
Mitral valve thickness (μm)
4 weeks, B.g7
4 weeks, K/B.g7
8 weeks, B.g7
8 weeks, K/B.g7
12 weeks, B.g7
12 weeks, K/B.g7
20 weeks, B.g7
20 weeks, K/B.g7
D
K/B.g7 Cdh5-CreERT2 ROSAmTmG/+
E
mGFP+LYVE1- GFP+ cells per MV
B.g7
K/B.g7
Age (Weeks)

Figure S11

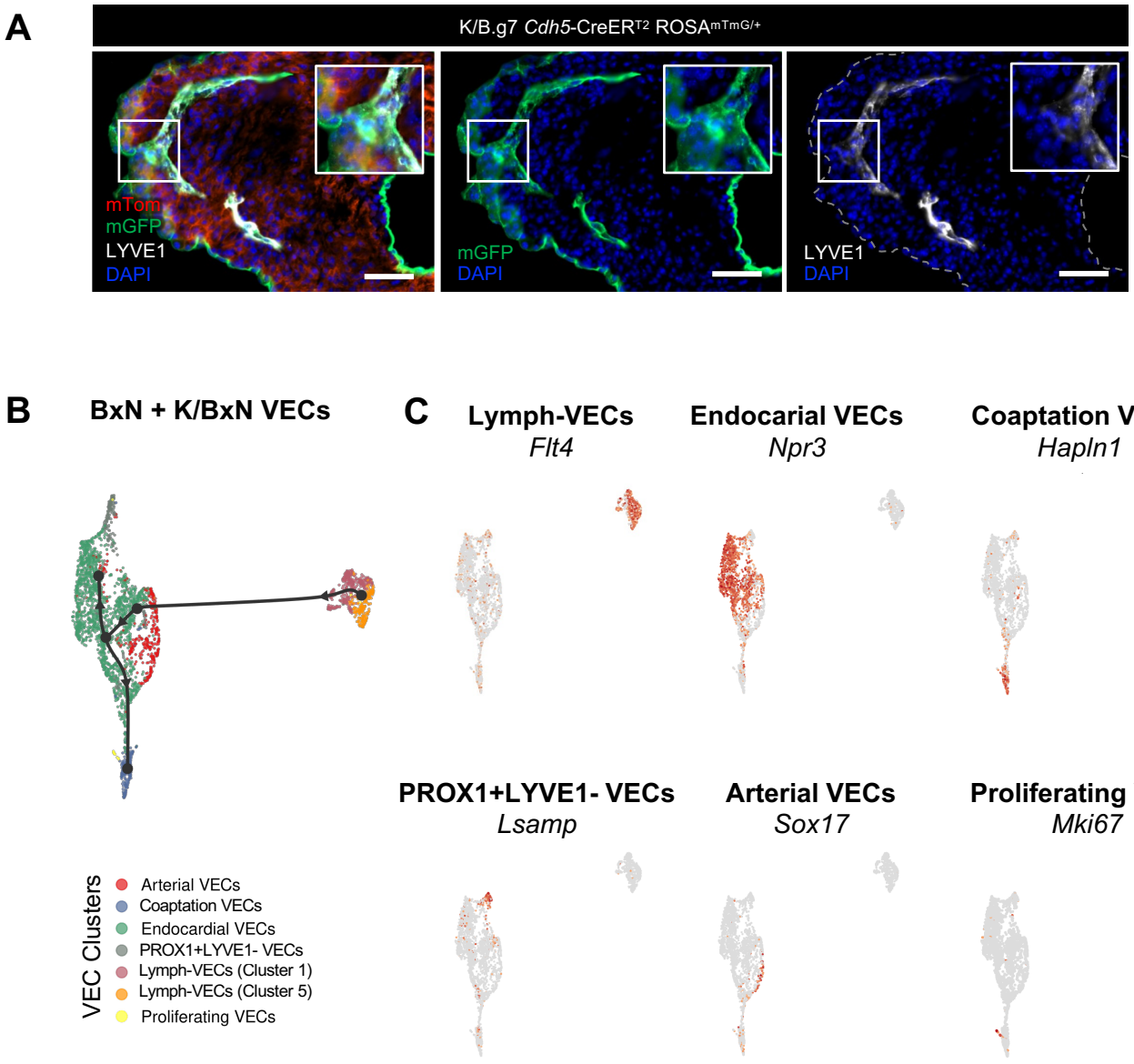
A
K/B.g7 Cdh5-CreERT2 ROSAmTmG/+
mTom
mGFP
LYVE1
DAPI
mGFP
DAPI
LYVE1
DAPI
B
BxN + K/BxN VECs
VEC Clusters
Arterial VECs
Coaptation VECs
Endocardial VECs
PROX1+LYVE1- VECs
Lymph-VECs (Cluster 1)
Lymph-VECs (Cluster 5)
Proliferating VECs
C
Lymph-VECs
Flt4
Endocarial VECs
Npr3
Coaptation VECs
Hapln1
PROX1+LYVE1- VECs
Lsamp
Arterial VECs
Sox17
Proliferating VECs
Mki67

Figure S12

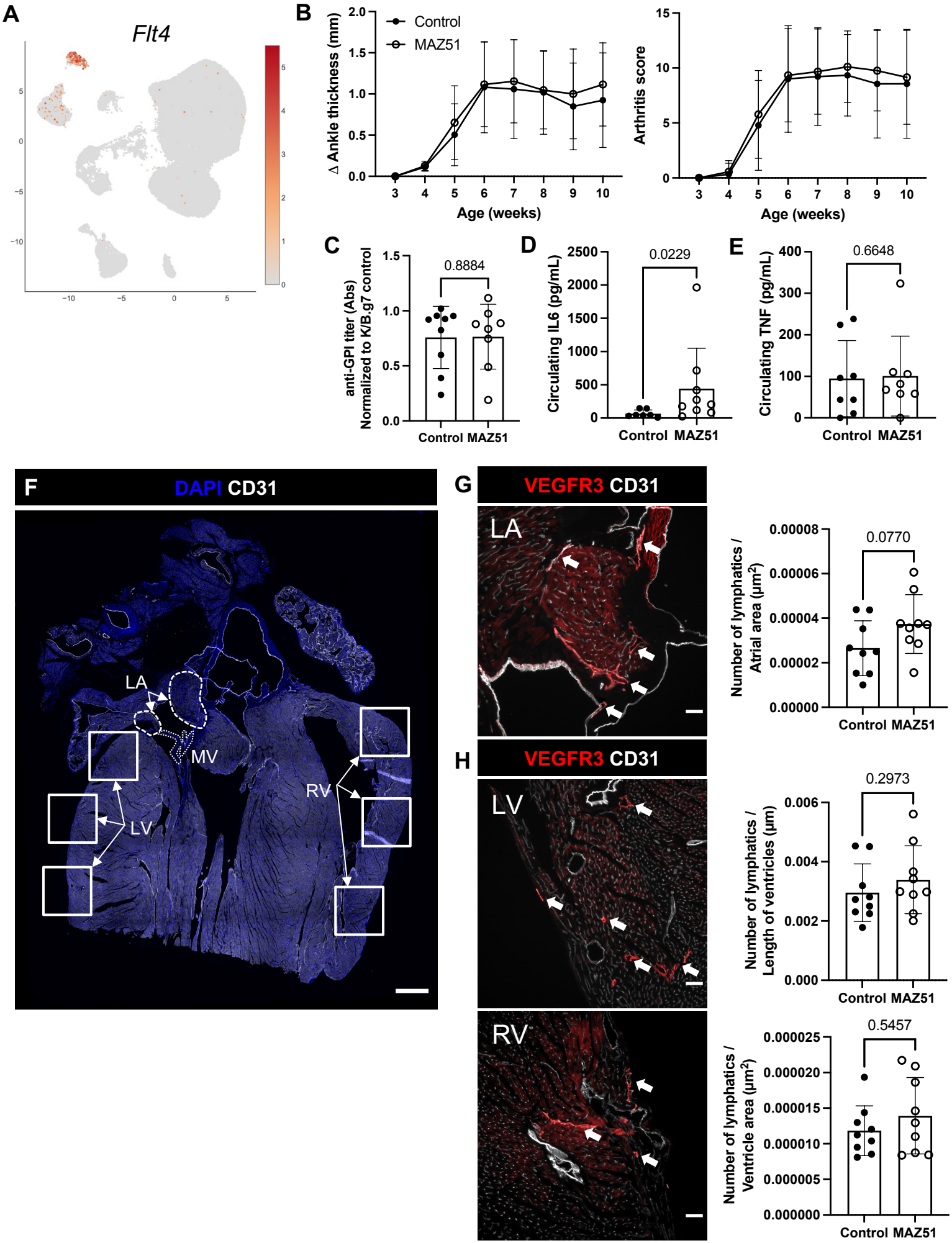
A
Flt4
B
Control
MAZ51
Δ Ankle thickness (mm)
Age (weeks)
Arthritis score
Age (weeks)
C
anti-GPI titer (Abs)
Normalized to K/B.g7 control
0.8884
Control MAZ51
D
Circulating IL6 (pg/mL)
0.0229
Control MAZ51
E
Circulating TNF (pg/mL)
0.6648
Control MAZ51
F
DAPI CD31
LA
MV
RV
LV
G
VEGFR3 CD31
LA
Number of lymphatics / Atrial area (μm²)
0.0770
Control MAZ51
H
VEGFR3 CD31
LV
Number of lymphatics / Length of ventricles (μm)
0.2973
Control MAZ51
RV
Number of lymphatics / Ventricle area (μm²)
0.5457
Control MAZ51

Figure S13

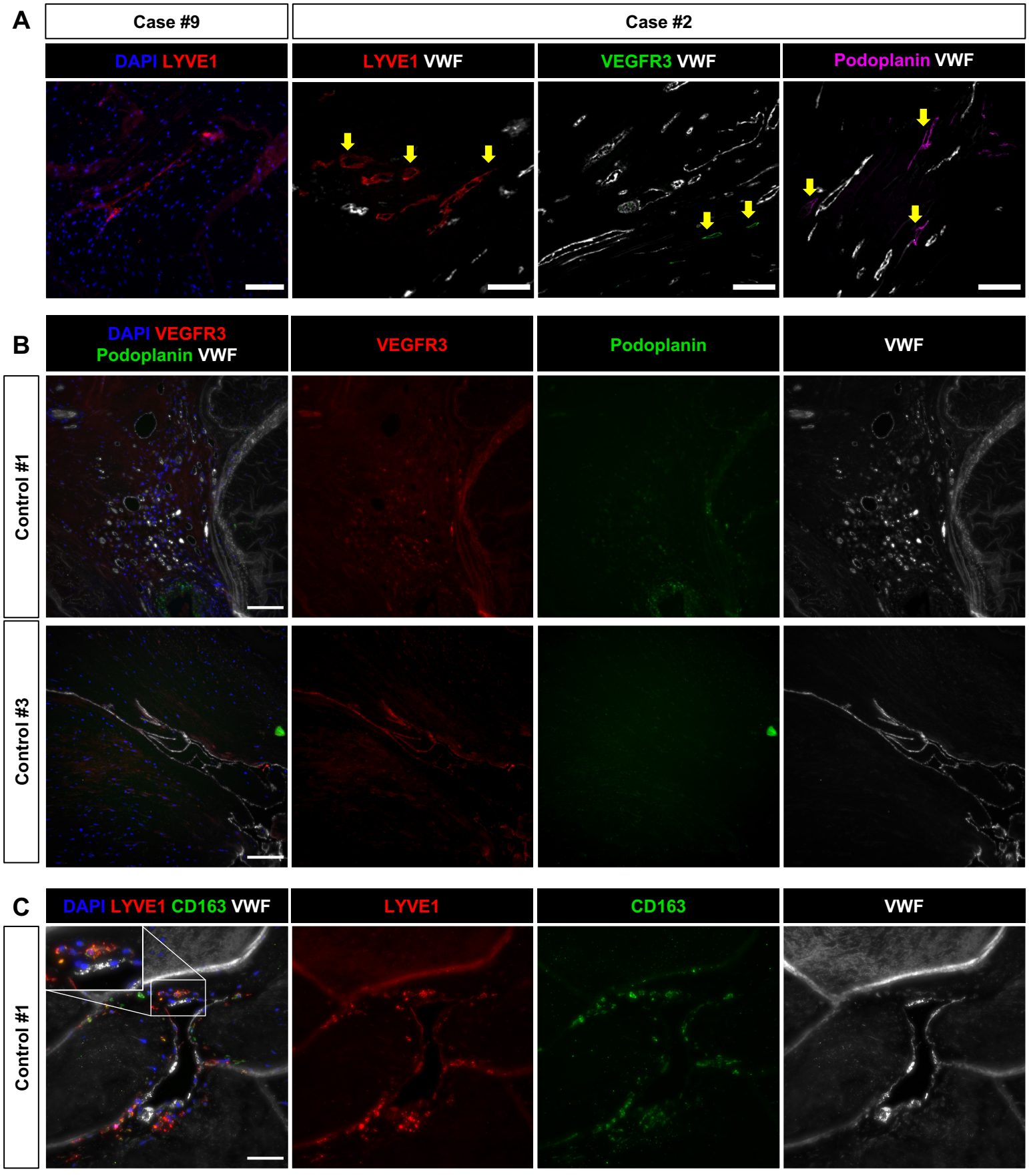
A
Case #9
Case #2
DAPI LYVE1
LYVE1 VWF
VEGFR3 VWF
Podoplanin VWF
B
DAPI VEGFR3
Podoplanin VWF
VEGFR3
Podoplanin
VWF
Control #1
Control #3
C
DAPI LYVE1 CD163 VWF
LYVE1
CD163
VWF
Control #1